Mathematisches Forschungsinstitut Oberwolfach

Report No. 36/2026

DOI: 10.4171/OWR/2026/36

Mini-Workshop: Stability and Bifurcations in PDE Models in Active Matter

Organized by
Leonid V. Berlyand, University Park
Tim Laux, Heidelberg
Anna Marciniak-Czochra, Heidelberg

16 August – 21 August 2026

Abstract. Active matter is characterised by its local consumption of energy, such as bacteria consuming nutrients when swimming. While most examples of active matter are biological in origin, there is growing interest in synthetic materials that exhibit active behaviour. The underlying PDE models in active matter may take various forms, often they are highly nonlinear, include free boundaries and possibly singularities. Unlike classical physical systems that are drawn to thermodynamic equilibrium, active systems are truly out of equilibrium. Hence classical equilibrium-based variational structures are often unavailable, creating a need for alternative analytical approaches, including novel asymptotic, spectral and computational techniques. Furthermore, central questions of bifurcation, stability and pattern formation give rise to non-self-adjoint or non-compact problems with subtle spectral properties.

Mathematics Subject Classification (2020): 35B52, 35B35, 35B36, 92C05, 92C10, 92C15, 92C17.

License: Unless otherwise noted, the content of this report is licensed under CC BY SA 4.0.

Introduction by the Organizers

Active matter systems are characterised by the local consumption of energy to generate motion or forces, ranging from swimming bacteria to cellular tissues and the actomyosin cytoskeleton, where cells generate stresses and structures self-organise. While most active matter is biological in origin, there is growing interest in synthetic materials exhibiting similar behaviour. Partial differential equations (PDEs) provide a versatile mathematical framework for modelling these systems, capturing both mechanical and biochemical processes and explaining the emergence of complex structures from underlying dynamics. Examples include cell migration,

which can be described by active gel theory as a symmetry breaking in actin flow, and tissue patterning arising from coupled mechanochemical systems. PDE models in active matter are often highly nonlinear, may involve free boundaries, and can exhibit singularities. Unlike classical physical systems, which tend towards thermodynamic equilibrium, active systems are intrinsically out of equilibrium. Consequently, classical variational methods are generally inapplicable, motivating the development of novel asymptotic techniques. Central questions of bifurcation, stability, and pattern formation often lead to non-self-adjoint or non-compact problems with subtle spectral properties leading to challenging mathematical questions. Despite recent progress, many theoretical and computational challenges remain: deriving rigorous PDE models linking processes across different scales, understanding the emergence and stability of patterns, and establishing general frameworks for non-equilibrium dynamics. Pushing these limits, we face a wide spectrum of mathematical questions in the analysis, computation and control of active matter systems.

Recent years have seen several breakthroughs at the interface of mathematics, physics, biology, and bioengineering in the study of active matter. Novel mathematical approaches now enable rigorous analysis of pattern formation, bifurcation, and stability in non-equilibrium systems, while cutting-edge experimental and computational techniques provide rich data and inspiration for modelling. At the same time, many fundamental questions remain open, including the rigorous derivation of PDE models across scales, the understanding of emergent behaviours in complex networks of interacting agents, and the development of general frameworks for stability and robustness in active systems. This workshop gave a timely opportunity to bring together key researchers, foster collaborations, and set the agenda for future research directions.

To foster synergies and challenge current approaches, the workshop went beyond traditional lectures on model analysis and advancements in mathematical methods. In addition to talks by mathematicians, the programme included lectures by distinguished biophysicists working on different aspects of active matter, covering the organisation and dynamics of individual cells, the collective behaviour of many-particle systems, and self-organisation and patterning in multicellular systems, or even whole ecosystems. These lectures integrated discrete and continuous structures across multiple spatial and time scales, linking them with system-level dynamics and providing a bridge between experimental observations and mathematical techniques.

The workshop covered systems ranging from single cells to ecosystems, with common threads being their rigorous formulation in terms of partial differential equations and the interest in the underlying pattern formation, bifurcation and stability analysis. Starting on the smallest represented scale, free boundary models for cell migration were introduced by Schwarz, with an overview of the analysis by Berlyand, and recent computer-assisted bifurcation and stability results presented by Safsten. Minimal models describing regeneration (as seen for example in Hydra and planaria) can lead to intricate patterns, as was presented by Stevens and

Popović. The precise bifurcation and stability behaviour of a mechanochemical model for Hydra was analysed by Cygan. Veerman used geometric singular perturbation theory to show pattern formation for similar models, in which curvature effects play the role of the long-range inhibitor to produce several patterns. Blanch-Mercader presented variational models describing the interplay between geometry and nematic order in deformable biological surfaces. Schmidtchen presented singular-limit results for nonlinear diffusion models and their connection to free-boundary problems. Safsten introduced a spatial predator-prey model, in which the predator and prey occupy different spatial domains, leading to non-standard bifurcation behaviour. Doelman presented PDE models for ecosystems, whose bifurcation behaviour may differ drastically from related ODE models, showcasing the importance of spatial structure in these systems. Lively discussions paved the way for future collaborations in active matter. Finally, to understand fundamental principles of active systems, Truskinovsky introduced a minimal dispersive, active model that exhibits travelling wave solitons by transforming chemical signals into mechanical work.

Acknowledgement: The MFO and the workshop organizers would like to thank the National Science Foundation for supporting the participation of junior researchers in the workshop by the grant DMS-2230648, "US Junior Oberwolfach Fellows".

Mini-Workshop: Stability and Bifurcations in PDE Models in Active Matter

Table of Contents

Ulrich S. Schwarz (joint with Oliver M. Drozdowski, Nils O. Winkler, Valentin Wössner, Falko Ziebert)
1D PDE-models for crawling cells 7

Alex Safsten (joint with Henri Berestycki, William F. Fagan)
A PDE model for predator–prey dynamics in mismatched domains 9

Angela Stevens (joint with Arnd Scheel, Christoph Tenbrock)
Active matter – functional principles in biological model systems 11

Markus Schmidtchen (joint with Tomasz Dębiec, Valentin V. Neumann)
On the viscous mesa limit 15

Marko Popović
Organizer organization in Hydra regeneration 17

Szymon Cygan (joint with Anna Marciniak-Czochra, Finn Münnich, Dietmar Oelz)
Pattern selection in mechanochemical model of pattern formation 18

Arjen Doelman
Singular patterns & ecosystem resilience 20

Frits Veerman
Mechanochemical pattern formation: far-from-equilibrium patterns on a deforming surface 22

Blanch-Mercader, Carles (joint with D. J. G. Pearce, C. Thibault, Q. Chaboche. Experimental results in the second part are due to T. L. A. Nguyen, F. C. Tsai)
Conical Surface Minimizers in Variational Models of Biofilms 23

Leonid Berlyand (joint with Oleksii Krupchytskyi, Tim Laux, Volodymyr Rybalko, Alex Safsten, Elina Soskina)
Stability and Bifurcations in a Free Boundary PDE Models of Cell Motility 25

Alex Safsten (joint with Leonid Berlyand, Oleksii Krupchytskyi, Tim Laux, Elina Soskina)
Numerysis: A numerical–analytic route to rigorous bistability in a cell-motion model 26

Lev Truskinovsky
Active Solitons 28

Abstracts

1D PDE-models for crawling cells

Ulrich S. Schwarz
(joint work with Oliver M. Drozdowski, Nils O. Winkler, Valentin Wössner, Falko Ziebert)

Motility is an essential capability of most biological cells and different cell types have evolved different strategies to move in their natural environments. While many single-living algae and bacteria use rotating flagella to swim with typical speeds of 100 μm/s, most animal cells move by crawling (the main exception being sperm cells, which swim with beating flagella). Crawling means that the cells are all the time in contact with a surface, and that they continuously extend the cell front and retract the cell back. This requires some kind of cyclic flow of cellular material, which means that hydrodynamic theories are required to model cell crawling. In addition, cell crawling is active and therefore requires some kind of energy input. In this contribution, we review the state-of-the-art to describe cell crawling by active gel theory, which is a hydrodynamic theory augmented by active stresses [1]. Because crawling is limited by the polymerization and turnover of the so-called actin cytoskeleton inside cells, the typical speed that can be achieved for crawling is only 1 μm/min. However, this is not a severe limitation for our body, which can perform most of its functions without cell migration. Cell migration is needed mainly during development, immune response and wound healing, which are slow processes.

While pioneering work on applying active gel theory to crawling focused on the effect of flow generated at the advancing front by actin polymerization [2], later it was shown that motor-based contractility in the bulk is sufficient to generate motility [3], in agreement with the experimental observation that myosin molecular motors are essential for cell crawling. The mathematical structure of this problem emerges as follows. First one assumes that stress σ has both a passive and an active contribution, and that the active one is generated by myosin motors with concentration c. Assuming the constitutive relation for a simple fluid, one has $\sigma = \eta\,\partial_x v + \chi c$, where v is flow velocity. Assuming linear friction with the substrate, $\partial_x \sigma = \xi v$, one gets

$$\mathcal{Z}\,\partial_{xx}\sigma - \sigma = -\mathcal{P}c \tag{1}$$

with $\mathcal{Z} \sim \eta/\xi$ and $\mathcal{P} \sim \chi$. For the concentration field, one writes an advection-diffusion equation:

$$\partial_t c + \partial_x(cv) = \partial_x(D\partial_x c) \tag{2}$$

with the diffusion constant D. Usually one considers a one-dimensional situation, corresponding to a cell migrating on a line or in a channel. This system of two PDEs has the structure of the Keller-Segel model for chemotaxis and has a relatively complex bifurcation structure. There exists one stable motile solution, which however has a strongly localized peak in motor concentration at the rear, which is

not physiological. Different processes exist in cells which lead to non-linear terms that can regularize these profiles, including biochemical saturation and non-linear diffusion [4, 5].

In order to model the fact that motor activity results from supramolecular motor complexes which assemble inside the cell, we have suggested that one can use the physics of the supercritical van der Waals fluid [6]. Using arguments either from reaction kinetics or linear irreversible thermodynamics, one arrives at a concentration dependent diffusion constant:

$$\mathcal{D}(c) = D\left[\left(1+\frac{c}{c_\infty - c}\right)^2 - e_\mathrm{A} c\right] \tag{3}$$

where c_∞ and e_A represent excluded volume and attraction, respectively. A bifurcation analysis shows that this model leads to realistic motor profiles. More importantly, it also leads to a subcritical pitchfork bifurcation and therefore to bistability between sessile and motile solutions, as observed experimentally. Recently, it has been shown that the curvature at the bifurcation point can be calculated analytically in a 2D version of this model [7].

In cells, there are not only one, but several types of myosin motors. A division of labor seems to exist between a fast type (non-muscle myosin IIA), that only generates small forces, and a slow type (non-muscle myosin IIAB), that generates large forces, roughly corresponding to the requirements of a dynamic front and a strong rear for migrating cells. Using the same strategy as for one motor type, one can derive an expanded model for cell crawling with two types of motors, and therefore with three PDEs [8]. Indeed, one finds that fast and slow motors localize to front and back, respectively. More interesting, though, the model also predicts the possibility of a Hopf bifurcation to an oscillatory solution, where motors continuously exchange positions and the cell continuously changes direction.

Overall, a picture emerges in which two fields and some kind of non-linearity are required to obtain stable and realistic motile solutions. While the first field is naturally the flow of the cytoskeleton (or, equivalently in active gel theory with frictional coupling, the stress), the second field does not need to be motor concentration. Recently we showed that motile solutions and bistability can also be obtained if the second field represents the concentration of the adhesion molecules that connect the crawling cell to the substrate [9]. In this case, the non-linearity is provided by the Bell-Dembo rates for the rupture of adhesions under force. In general, the body of work discussed here shows that the molecular properties of biological systems often translate into non-linear mathematical properties on the PDE-level that also can be understood from thermodynamic principles. This provides a rigorous way to derive macroscopic models from known microscopic processes.

References

[1] Frank Jülicher, Stephan W Grill, and Guillaume Salbreux, *Hydrodynamic theory of active matter*, Reports on Progress in Physics **81** (2018), 076601.

[2] K Kruse, J F Joanny, F Jülicher, and J Prost, *Contractility and retrograde flow in lamellipodium motion*, Physical Biology **3** (2006), 130.
[3] P. Recho, T. Putelat, and L. Truskinovsky, *Contraction-Driven Cell Motility*, Physical Review Letters **111** (2013), 108102.
[4] Pierre Recho, Thibaut Putelat, and Lev Truskinovsky, *Mechanics of motility initiation and motility arrest in crawling cells*, Journal of the Mechanics and Physics of Solids **84** (2015), 469–505.
[5] H. Chelly and P. Recho, *Cell motility as an energy minimization process*, Physical Review E **105** (2022), 064401.
[6] Oliver M. Drozdowski, Falko Ziebert, and Ulrich S. Schwarz, *Optogenetic control of migration of contractile cells predicted by an active gel model*, Communications Physics **6** (2023), 1–12.
[7] Leonid Berlyand, Oleksii Krupchytskyi, and Tim Laux, *Change of Bifurcation Type in 2D Free Boundary Model of a Moving Cell with Nonlinear Diffusion*, Journal of Nonlinear Science **36** (2026), 95.
[8] Nils O. Winkler, Oliver M. Drozdowski, Falko Ziebert, and Ulrich S. Schwarz, *Active gel theory for cell migration with two myosin isoforms*, Physical Review E **112** (2025), 024413.
[9] Valentin Wössner, Oliver M Drozdowski, Falko Ziebert, and Ulrich S Schwarz, *Active gel model for one-dimensional cell migration coupling actin flow and adhesion dynamics*, New Journal of Physics **26** (2024) 073039.

A PDE model for predator–prey dynamics in mismatched domains

Alex Safsten
(joint work with Henri Berestycki, William F. Fagan)

Many predator–prey models assume that both species occupy the same spatial region. In applications this need not be true: prey may have access to a refuge from which predators are excluded, while terrestrial predators may concentrate their activity on trails or separated hunting ranges inside a larger prey habitat. We therefore let the prey density u be defined on a bounded domain $\Omega \subset \mathbb{R}^n$, while the predator density v is defined only on a subdomain $A \subset \Omega$. The complement $\Omega \setminus A$ is a predator-free exclusion zone. We consider

$$\begin{cases} u_t - d_u \Delta u = f(u) - \beta \mathbf{1}_A uv, & x \in \Omega, \\ v_t - d_v \Delta v = (\alpha u - \gamma) v, & x \in A, \\ \partial_\nu u = 0, & x \in \partial\Omega, \\ \partial_\nu v = 0, & x \in \partial A, \end{cases} \tag{1}$$

with positive parameters. The prey growth term has a strong Allee effect; a typical example is $f(u) = u(u-\theta)(1-u)$, $0 < \theta < 1$. Thus sufficiently heavy predation can push the prey below the Allee threshold and ultimately cause extinction of both species. The question is how the size and geometry of A affect coexistence and predator abundance. The results below are joint work with Henri Berestycki and William F. Fagan; see [1].

Protection-zone models have previously been studied using persistence, bifurcation, and continuation methods; see, for example, [3, 2, 4]. A principal result in

our setting is a global existence theorem for coexistence equilibria. Assume $\gamma < \alpha$. There exists $R_0 > 0$ such that if, for some $\rho > 0$,

$$A \subset B_\rho \subset B_{\rho+R_0} \subset \Omega,$$

then the stationary version of (1) has a solution satisfying $0 < u < 1$ in Ω and $v > 0$ in A. Thus a sufficiently large predator-free region guarantees coexistence in any spatial dimension. The result is global: the coexistence state need not arise from a local bifurcation from a semi-trivial state.

The proof uses Leray–Schauder degree. A scalar bistable problem on the predator-free region first gives a lower barrier ζ for the prey and hence a natural search region $\zeta < u < 1$. A direct degree argument is obstructed by the boundary equilibrium $(u, v) = (1, 0)$. To remove it, let $\lambda[u]$ and $\phi[u]$ be the principal eigenvalue and a normalized positive principal eigenfunction of

$$-d_v\Delta - (\alpha u - \gamma)$$

on A with Neumann boundary conditions. At coexistence, $\lambda[u] = 0$ and $v = s\phi[u]$ for some $s > 0$. The two-function elliptic problem can therefore be recast as a zero of a Fredholm map in (u, s). The state $u \equiv 1$ is no longer a zero because $\lambda[1] = \gamma - \alpha \neq 0$. A boundary-root-free homotopy then reduces the degree to two elementary factors, each equal to one, so the original problem has a coexistence solution.

There is also a complementary nonexistence result. If $A = \Omega$, so that no refuge is present, then for sufficiently small predator mortality γ the stationary system has no coexistence equilibrium. Hence exclusion zones can be not only sufficient but, in some parameter regimes, necessary for persistence.

The opposite geometric limit is equally striking. In one dimension let $\Omega = (0, L)$ and $A = (0, a)$, and choose any coexistence equilibrium (u_a, v_a). For L sufficiently large, as $a \to 0$ every such selection has the same limit:

$$u_a \longrightarrow \bar{u}, \qquad v_a(x)\,dx \rightharpoonup M\delta_0, \qquad M = \frac{d_u\alpha}{\beta\gamma}\bar{u}'(0) > 0,$$

where

$$-d_u\bar{u}'' = f(\bar{u}), \qquad \bar{u}(0) = \frac{\gamma}{\alpha}, \qquad \bar{u}'(L) = 0.$$

Thus the predator density becomes singular as its habitat collapses, but its total mass remains positive. For a sufficiently regular branch, if $V(a) = \int_0^a v(x; a)\,dx$, then

$$\lim_{L\to\infty} V'(0) = \frac{2\alpha}{3\beta\gamma} f\left(\frac{\gamma}{\alpha}\right).$$

In particular, if $\gamma/\alpha < \theta$, then $V'(0) < 0$: making a zero-width predator region slightly wider initially *decreases* predator abundance. For sufficiently efficient predators, thinner can genuinely be better.

Preliminary numerical experiments suggest much richer behavior away from these asymptotic regimes. In one dimension, varying the width of the predator region produces equilibria, periodic attractors, and apparently chaotic dynamics, with Hopf and saddle-node bifurcations associated with abrupt extinction. In

two dimensions, simulations with two separated predator regions show that total populations can depend nonmonotonically on their separation and on proximity to the outer boundary. Natural next questions include shape optimization of A, higher-dimensional thin limits in which predator regions collapse to curves or interfaces, and a rigorous bifurcation analysis of the dynamics seen numerically.

References

[1] H. Berestycki, W. F. Fagan, and A. Safsten, *The influence of exclusion zones on the coexistence of predator and prey with an Allee effect*, preprint, arXiv:2602.21414 (2026).
[2] R. Cui, J. Shi, and B. Wu, *Strong Allee effect in a diffusive predator–prey system with a protection zone*, J. Differential Equations **256** (2014), 108–129.
[3] Y. Du and J. Shi, *A diffusive predator–prey model with a protection zone*, J. Differential Equations **229** (2006), 63–91.
[4] N. Min and M. Wang, *Dynamics of a diffusive prey–predator system with strong Allee effect growth rate and a protection zone for the prey*, Discrete Contin. Dyn. Syst. B **23** (2018), 1721–1737.

Active matter – functional principles in biological model systems

Angela Stevens
(joint work with Arnd Scheel, Christoph Tenbrock)

Planarians are nonparasitic flatworms commonly found in freshwater streams and ponds [2, 3] with a body size in the *mm*-scale. When small tissue parts are cut from the flatworm - in extreme cases just 0.5% of the original size - these can regenerate to a fully functioning and intact organism [2] with head and tail positioned such that the original orientation of the tissue fragment is respected. When tissue parts are cut from a donor and grafted into a host, the newly created planarian integrates the old positional information of the tissue fragment from the donor with the new positional information it obtains from the host. A better understanding of these processes has a far reaching potential for regeneration in general.

Based on experimental data, a system of reaction-diffusion equations for the regeneration of planarians is introduced and analyzed. We model dynamics of head and tail cells expressing positional control genes that translate into localized signals which in turn guide stem cell differentiation. Tissue orientation and positional information are encoded in a long range *wnt*-related signaling gradient. Our system correctly reproduces typical cut and graft experiments, and preserves polarity in regeneration over orders of magnitude in body size during growth phases. Key to polarity preservation in our model is the sensitivity of cell differentiation to gradients of *wnt*-related signals relative to the tissue surface. This process is particularly relevant in small tissue layers close to cuts during their healing, and modeled in a robust fashion through dynamic boundary conditions.

To the best of our knowledge, our system of reacting and diffusing species is to date the only model that correctly recovers most of the typical cutting and grafting experiments, and preserves polarity during regeneration, even of small tissue fragments.

The mathematical model. We focus on the ante-posterior (AP) axis of planarians and consider a one-dimensional domain $x \in [-L, L]$, populated by different cell types and signals. Head cells **h** and tail cells **d** generate corresponding signals $\mathbf{u_h}$ and $\mathbf{u_d}$, which activate the respective differentiation of stem cells **s**. A long-range *wnt*-related signal **w**, in short *wnt*-signal, encodes orientational information through its gradient. It is produced by tail cells in a saturating fashion, and degraded by reactions with head cells:

$$\partial_t s = D_s \partial_{xx} s + \rho_s(s) - p_h u_h s - p_d u_d s \ , \tag{1}$$

$$\partial_t h = D_h \partial_{xx} h + p_h u_h s - \eta_h h, \ , \tag{2}$$

$$\partial_t d = D_d \partial_{xx} d + p_d u_d s - \eta_d d \ , \tag{3}$$

$$\partial_t u_h = D_{u_h} \partial_{xx} u_h + h^2 (r_0 - r_1 u_h) - r_2 u_h d - r_3 u_h \ , \tag{4}$$

$$\partial_t u_d = D_{u_d} \partial_{xx} u_d + d^2 (r_0 - r_1 u_d) - r_2 u_d h - r_3 u_d \ , \tag{5}$$

$$\partial_t w = D_w \partial_{xx} w - p_w h w + p_w d(1 - w) \ . \tag{6}$$

Stem cells proliferate with saturating rate and undergo apoptosis [1], which is encoded in $\rho_s(s) = p_s \frac{s}{1+s} - \eta_s s$. Stem cells also differentiate irreversibly into head and tail cells, guided by positional control genes, which are modeled by the respective related localized signals u_h, u_d. Those signals are produced by head and tail cells up to a saturation level, with rates r_0 and r_1 and decay with rate r_3 . This interaction works during both, normal tissue turnover and regeneration [2]. Head and tail cells result from stem cell differentiation and do not proliferate. They undergo apoptosis and degrade the signal associated with the other cell type with rate r_2.

The quadratic dependence of the production of u_h and u_d on h and d corresponds to higher order molecular kinetics, quadratic here in their simplest form. Replacing these reactions by first-order kinetics, linear in h, d, would result in spontaneous growth of head and tail regions caused by a linear instability of the zero state. The quadratic dependence postulated here suppresses this instability and we suggest that some effective higher-order kinetics are indeed crucial there. We used the same parameter p_w for production and degradation of w, since differing rates showed qualitatively similar outcomes in our simulations. Finally, random motion of cells and diffusion of signal molecules are modeled through the diffusion coefficients D_j.

Writing $U(t,x) = (s, h, d, u_h, u_d, w)(t,x)$, $\mathcal{D} = \operatorname{diag}(D_s, D_h, D_d, D_{u_h}, D_{u_d}, D_w)$ and $\mathcal{F} = (F_s, F_h, F_d, F_{u_h}, F_{u_d}, F_w)$ in the system (1)–(6), we find

$$\partial_t U = \mathcal{D} U_{xx} + \mathcal{F}(U) \ . \tag{7}$$

We prescribe inhomogeneous Dirichlet boundary conditions $U_{x=\pm L} = U_\pm$ and evolution equations for the time dependent Dirichlet data

$$\frac{\mathrm{d}}{\mathrm{d}t} U_\pm = -\frac{1}{\gamma} \mathcal{D} \, \partial_\nu U|_{x=\pm L} + \mathcal{F}(U_\pm) + \mathcal{B} \ . \tag{8}$$

We think of $U_\pm$ as concentrations in a boundary compartment of length γ where concentrations are spatially constant. Fluxes $-\frac{1}{\gamma}\mathcal{D}\,\partial_\nu U|_{x=\pm L}$ ensure mass conservation up to kinetics,

$$\begin{aligned}\frac{\mathrm{d}}{\mathrm{d}t}\left(\int U + \sum_{\pm}\gamma U_\pm\right) &= \int \mathcal{F}(U) + \sum_{\pm}\left(\mathcal{D}\partial_\nu U|_{\pm L} + \gamma\frac{\mathrm{d}}{\mathrm{d}t}U_\pm\right)\\ &= \int \mathcal{F}(U) + \gamma\sum_{\pm}\left(\mathcal{F}(U_\pm) + \mathcal{B}\right).\end{aligned}$$

Kinetics here are identical to those in the bulk of the domain up to a new term $\mathcal{B}$, present in the dynamics for $s_\pm$, $h_\pm$, and $d_\pm$, that represents a boundary-specific stem-cell differentiation mechanism through rates $\Psi^\pm_{h/d}$,

$$\frac{\mathrm{d}}{\mathrm{d}t}s_\pm = -\frac{1}{\gamma}D_s\,\partial_\nu s|_{x=\pm L} + F_s - \Psi^\pm_h s - \Psi^\pm_d s\,, \tag{9}$$

$$\frac{\mathrm{d}}{\mathrm{d}t}h_\pm = -\frac{1}{\gamma}D_h\,\partial_\nu h|_{x=\pm L} + F_h + \Psi^\pm_h s\,, \tag{10}$$

$$\frac{\mathrm{d}}{\mathrm{d}t}d_\pm = -\frac{1}{\gamma}D_d\,\partial_\nu d|_{x=\pm L} + F_d + \Psi^\pm_d s\,. \tag{11}$$

The differentiation is triggered by lack of head or tail cells, and directed according to the sign of $\partial_\nu w$, explicitly through $\Psi^\pm_{h/d} = \Psi_{h/d}(h,d,\partial_\nu w)|_{x=\pm L}$,

$$\Psi_h = \tau(1-h)(1-d)\chi^\varepsilon_{>\theta}(\partial_\nu w), \quad \text{and} \quad \Psi_d = \tau(1-h)(1-d)\chi^\varepsilon_{<-\theta}(\partial_\nu w).$$

Here $\tau \gg 1$ is the rate of differentiation, and the χ^ε are smoothed versions of the characteristic function, for example

$$\begin{aligned}\chi^\varepsilon_{>\theta}(\xi) &= \frac{1}{2}\Big[\tanh((\xi-\varepsilon\theta)/\varepsilon)+1\Big]\,,\\ \chi^\varepsilon_{<-\theta}(\xi) &= \frac{1}{2}\Big[\tanh(-(\xi+\varepsilon\theta)/\varepsilon)+1\Big]\,;\end{aligned} \tag{12}$$

The steepness ε^{-1} of the smoothed characteristic function can be interpreted as a sensitivity of differentiation with respect to small gradients. The offset θ measures minimal detectable strength of the gradient at the body or wound edge in ε-units. Overall, the kinetics F_s in (1) regulate a near-constant supply of stem-cells. As a result, a healthy planarian consists of a high concentration of h near $x=-L$, a high concentration of d near $x=L$, and a near-constant gradient of w in $x\in(-L,L)$.

Eliminating stem cells and short-range signals. Proliferation of stem cells in (1) is much faster than differentiation, $p_s = 200$, $p_h = p_d = 1$. Thus equilibrium concentrations depend only marginally on differentiation, that is, on the concentrations of $u_{h/d}$. Solving for equilibria by setting $\rho_s(s) = 0$, we obtain $s = (p_s - \eta_s)/\eta_s$ which in our choice of parameters gives $s \equiv 1$. Our simulations all support this approximation. Having set $s \equiv 1$, we notice that the signal production rates r_j are larger than the cell differentiation and death rates $p_{h/d}$ and $\eta_{h/d}$. Using an

adiabatic reduction for the kinetics, one then equilibrates the reaction rates for $u_{h/d}$ and finds $u_{h/d}$ as functions of h and d,

$$u_h = \frac{r_0 h^2}{r_1 h^2 + r_2 d + r_3}, \qquad u_d = \frac{r_0 d^2}{r_1 d^2 + r_2 h + r_3}. \tag{13}$$

Similar to the case of stem cell dynamics, the reduction for the kinetics is valid under suitable bounds on gradients, and such reduced systems capture the key structure of the dynamics quite well. In summary, we obtain

$$\begin{aligned}
\partial_t h &= D_h \partial_{xx} h + p_h \frac{r_0 h^2}{r_1 h^2 + r_2 d + r_3} - \eta_h h \ , \\
\partial_t d &= D_d \partial_{xx} d + p_d \frac{r_0 d^2}{r_1 d^2 + r_2 h + r_3} - \eta_d d \ , \\
\partial_t w &= D_w \partial_{xx} w - p_w h w + p_w d(1-w) \ , \text{ with boundary data} \\
\frac{\mathrm{d}}{\mathrm{d}t} h_\pm &= -\frac{1}{\gamma} D_h \partial_\nu h_\pm + p_h \frac{r_0 h_\pm^2}{r_1 h_\pm^2 + r_2 d_\pm + r_3} - \eta_h h_\pm + \Psi_h^\pm \ , \\
\frac{\mathrm{d}}{\mathrm{d}t} d_\pm &= -\frac{1}{\gamma} D_d \partial_\nu d_\pm + p_d \frac{r_0 d_\pm^2}{r_1 d_\pm^2 + r_2 h_\pm + r_3} - \eta_d d_\pm + \Psi_d^\pm \ , \\
\frac{\mathrm{d}}{\mathrm{d}t} w_\pm &= -\frac{1}{\gamma} D_w \partial_\nu w_\pm - p_w h_\pm w_\pm + p_w d_\pm (1-w_\pm) \ , \text{ where again} \\
&\quad \Psi_h(h,d,\partial_\nu w) = \tau(1-h)(1-d)\chi^\varepsilon_{>0}(\partial_\nu w) \ , \\
&\quad \Psi_d(h,d,\partial_\nu w) = \tau(1-h)(1-d)\chi^\varepsilon_{<0}(\partial_\nu w) \ .
\end{aligned} \tag{14}$$

Simulations of this reduced model are almost indistinguishable from the full model.

This talk is based on [4] and [5].

References

[1] J. Baguñà, R. Romero, E. Saló, J. Collet, C. Auladell, M. Ribas, M. Riutort, J. García-Fernàndez, F. Burgaya, and D. Bueno. *Growth, degrowth and regeneration as developmental phenomena in adult freshwater planarians.* In *Experimental embryology in aquatic plants and animals*, Springer (1990), pages 129–162.

[2] P. W. Reddien and A. S. Alvarado, *Fundamentals of planarian regeneration.* Annu. Rev. Cell Dev. Biol. **20** (2004), 725–757.

[3] J. C. Rink. *Stem Cells, Patterning and Regeneration in Planarians: Self-Organization at the Organismal Scale*, Springer, New York, (2018), 57–172.

[4] A. Scheel, A. Stevens and C. Tenbrock, *Signaling gradients in surface dynamics as basis for planarian regeneration* J. Math. Biol. **83**, No. 1 (2021), Paper No. 6.

[5] C. Tenbrock. *Mathematical models for regeneration on the example of planarians.* PhD-Thesis, University of Münster, Germany (2017).

On the viscous mesa limit

Markus Schmidtchen
(joint work with Tomasz Dębiec, Valentin V. Neumann)

Several challenging singular-limit problems involving degenerate parabolic equations ensued the existence theory of the filtration equation in [2, 1]. A particularly fascinating example is the so-called *mesa problem*. For the sake of brevity, we refer to [3] for a nod to the mathematical history and contemporary results. To introduce the mathematical question, consider the porous medium equation

$$\partial_t \rho = \Delta \rho^m, \tag{1}$$

with exponent $m \geq 2$, equipped with some nonnegative initial data, ρ_0. Clearly, solutions to Eq. (1) depend on the exponent m. Then, the *mesa limit* consists of letting $m \to \infty$ in the equation. To gain some intuition, we write

$$\partial_t \rho = \Delta \rho^m = \operatorname{div}(m\rho^{m-1}\nabla\rho) = \operatorname{div}(D_m(\rho)\nabla\rho).$$

For $m \approx \infty$, the diffusion constant behaves like

$$D \approx \begin{cases} 0, & \text{on } \{\rho < 1\}, \\ \infty, & \text{on } \{\rho > 1\}, \end{cases} \tag{2}$$

i.e., solutions diffuse infinitely fast if their density value surpasses unity and, otherwise, do not move at all. In particular, the limit density satisfies $0 \leq \rho \leq 1$, resulting in time-stationary, spatially flat-topped profiles. Their resemblance with some flat-topped mountain ranges found in the US then gave rise to the name *mesas*.

The addition of a zeroth order term modelling, e.g., growth dynamics, qualitatively changes the behaviour [4]: Rather than a stationary profile, the limit solution solves a free-boundary problem of Hele-Shaw type. To understand the quality of this limit, it is customary to write the equation as conservation law

$$\partial_t \rho_m + \operatorname{div}(\rho_m v_m) = \rho_m G(p_m), \tag{3a}$$

where the velocity field, v_m, is related to the pressure, p_m, through Darcy's law

$$v_m = -\nabla p_m, \qquad p_m := \frac{m}{m-1}(\rho_m)^{m-1}. \tag{3b}$$

A short computation reveals that

$$\partial_t p_m = |\nabla p_m|^2 + (m-1)p_m(\Delta p_m + G(p_m). \tag{4}$$

Formally, letting $m \to \infty$, in Eq. (4), one obtains an obstacle-type problem

$$0 = p_\infty(\Delta p_\infty + G(p_\infty)), \tag{5}$$

such that either $p_\infty = 0$ or $\Delta p_\infty + G(p_\infty) = 0$ on $\{p_\infty > 0\}$. It can be shown that the saturation zone coincides with the set of positive pressure $\{\rho_\infty = 1\} = \{p_\infty > 0\}$, and that this set evolves with a normal outward velocity $-\nabla p_\infty \cdot \nu$. The growth of the domain encapsulated by the free boundary is driven by the mass generated by the growth term and the incompressibility condition $0 \leq \rho_\infty \leq 1$.

The viscous mesa problem, suggested in [5], replaces Darcy's law by the elliptic Brinkman law modelling velocity dissipation due to viscosity

$$-\nu\Delta v + v = -\nabla p, \tag{6}$$

such that Darcy's law is recovered for vanishing viscosity, $\nu \to 0$. Until now, existing results require initial data to (1) be (or converge to) indicators of compact sets, (2) have $L^1 \cap L^\infty$ regularity, and (3) the limit objects themselves are compactly supported $L^1 \cap L^\infty$-objects. In this talk (based on [6]), we show that

(1) **any sequence** of $L^1 \cap L^q$-data ($q = \max(2, d/2)$)
(2) whose union of supports is only required to **have finite measure** rather than being compact
(3) passes to a limit that is **time continuous** and $\boldsymbol{L^\infty}$ in space and time,
(4) which satisfies the known **complementarity relations** in the **presence of mushy regions**,

unveiling that L^∞-regularity is not merely a consequence of propagation of boundedness but intrinsically tied to the mesa limit.

We prove the viscous mesa limit under this milder set of assumptions while proving better regularity, building on the nonlocal compactness method [7]. A careful study of the dissipation along solutions produced by their nonlocal quantity is shown to encode some spatial compactness of the pressure. Furthermore, the L^∞-assumption on initial data is removed by introducing weights that penalise trajectories where the velocity loses sufficient regularity cf. [8]. Furthermore, we prove a technical lemma of Aubin-Lions-Simons style that marries the uniform-in-time oscillation control with the negative Sobolev control of time derivatives of a family to infer its precompactness in $L^\infty(K \times (0,T))$, for any compact K. Finally, the L^∞ regularising effect is an algebraic necessity coming from having integrable data.

References

[1] E. S. Sabinina, *On the Cauchy problem for the equation of nonstationary gas filtration in several space variables*, Soviet Math. Dokl. **2** (1961), 166–169.

[2] O. A. Oleĭnik, A. S. Kalashnikov, and Yu-lin Zhou, *The Cauchy problem and boundary problems for equations of the type of non-stationary filtration*, Izv. Akad. Nauk SSSR, Ser. Mat. **22** (1958), 667–704.

[3] N. David and M. Schmidtchen, *On the incompressible limit for a tumour growth model incorporating convective effects*, Commun. Pure Appl. Math. **77** (2024), 2613–2650.

[4] B. Perthame, F. Quirós, and J. L. Vázquez, *The Hele–Shaw asymptotics for mechanical models of tumor growth*, Arch. Ration. Mech. Anal. **212** (2014), 93–127.

[5] B. Perthame and N. Vauchelet, *Incompressible limit of a mechanical model of tumour growth with viscosity*, Philos. Trans. R. Soc. A Math. Phys. Eng. Sci. **373** (2015), 20140283.

[6] T. Dębiec, V. V. Neumann, and M. Schmidtchen, *Incompressible limit for a two-species Brinkman model with drift*, arXiv preprint arXiv:2608.27686 (2026).

[7] F. Ben Belgacem and P.-E. Jabin, *Compactness for nonlinear continuity equations*, J. Funct. Anal. **264** (2013), 139–168.

[8] D. Bresch and P.-E. Jabin, *Global existence of weak solutions for compressible Navier–Stokes equations: thermodynamically unstable pressure and anisotropic viscous stress tensor*, Ann. of Math. **188** (2018), 577–684.

Organizer organization in *Hydra* regeneration

Marko Popović

The freshwater polyp *Hydra* can regenerate an entire animal from a small excised tissue fragment. The fragment seals into a fluid-filled spheroid whose supracellular actomyosin fibers recover nematic order as a new body axis forms. Instead of the generic passive configuration of four $+1/2$ defects on a sphere, a $+1$ defect forms at the future head and two $+1/2$ defects remain near the future foot. The head defect co-localizes with the Wnt-associated head organizer, suggesting a shared mechanism for structural and biochemical patterning.

Live imaging by Maroudas-Sacks et al. revealed recurring episodes of strong stretching and rupture from the onset of regeneration [1], driven by transient contractions of the ectodermal fibers. Radial fibers around an aster focus area strain at its core; a $+1/2$ pair focuses strain less efficiently, and little focusing occurs in uniformly aligned regions. The strongest events occur at the future head, and the primary focusing site is identifiable early, where the organizer later emerges.

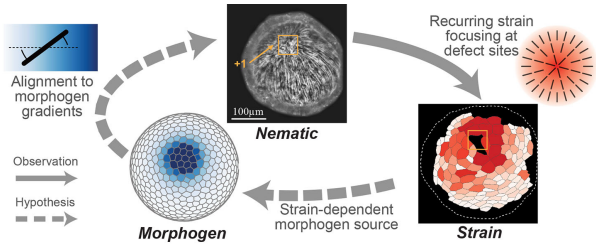

Figure 1. Proposed feedback loop for formation of the head organizer. Radial actomyosin fibers form a $+1$ nematic defect. Their transient contraction focuses tissue strain at the defect core (solid arrow; observed experimentally). Local dilation is proposed to initiate a morphogen source. Its concentration gradient aligns the fibers radially and stabilizes the $+1$ defect (dashed arrows; hypothesized), closing the loop. Adapted from [1].

To isolate the consequences of the proposed feedback loop, we extract from it a minimal model in which the tissue is an elastic medium with strain ϵ_{ij}, nematic tensor q_{ij}, and morphogen concentration c:

$$\begin{aligned} \partial_j \sigma_{ij} &= 0, \qquad \sigma_{ij} = 2\mu\epsilon_{ij} + B\epsilon_{kk}\delta_{ij} + \zeta q_{ij}, \\ \partial_t c &= D_c \nabla^2 c - a_- c + a_+ H(\epsilon_{kk} - \epsilon_{\mathrm{th}}), \\ \partial_t \theta &= D_\theta \nabla^2 \theta + \alpha |\nabla c|^2 \sin[2(\theta - \phi)]\,, \end{aligned} \tag{1}$$

Here σ_{ij} is stress, ϵ_{ij} linear strain, ϵ_{kk} areal strain, μ and B the shear and bulk moduli, and δ_{ij} the identity. The tensor q_{ij} gives fiber orientation and $\zeta > 0$ the

contractile active-stress amplitude. The morphogen c has diffusivity D_c, degradation rate a_-, and production amplitude a_+; the Heaviside function H selects $\epsilon_{kk} > \epsilon_{\mathrm{th}}$. The angle θ relaxes with orientational diffusivity D_θ, ϕ is the direction of ∇c, and α is the gradient-alignment strength. Repeated spatial indices are summed and ∂_j denotes differentiation.

For a radial $+1$ defect, active stress produces maximal isotropic strain near the core. The resulting morphogen source and radial gradient make the aster a self-consistent steady state. The controls are the effective threshold $\epsilon_{\mathrm{th}}/\bar{\zeta}$, with $\bar{\zeta} = \zeta/(B + 2\mu)$, and relative alignment strength $S = \alpha a_+^2/(a_-^2 D_\theta)$.

Nematic elasticity favors splitting a $+1$ defect into two $+1/2$ defects. Their separation is governed by Coulomb-like repulsion opposed by attraction from the morphogen gradient. As S increases, two fold bifurcations delimit a bistable regime of separated and bound states. At strong coupling only the bound state remains, with dimensionless steady separation $\bar{d}^* = d^*/R$ (d^* is the defect separation and R the system radius) scaling as $S^{-1/4}$, and critical coupling S_c satisfying $\log S_c \sim (\epsilon_{\mathrm{th}}/\bar{\zeta})_c$. Vertex-model simulations recover this phase structure and scaling, with discreteness-dependent shifts [2].

Taken together, the results show that the proposed feedback can stabilize a $+1$ nematic defect together with a localized morphogen source, providing a possible physical basis for their co-localization at the head organizer. More generally, they suggest that tissue mechanics, biochemical signaling, and nematic order may act together during regeneration. How the relevant couplings are implemented molecularly, and how the organizer first emerges, remain open questions.

References

[1] Y. Maroudas-Sacks, S. Senthilkumar, L. Garion, Y. Ascoli-Abbina, A. Westfried, N. Dori, I. Pasvinter, M. Popović, and K. Keren, *Mechanical strain focusing at topological defect sites in regenerating Hydra*, Development **152** (2025), dev204514.

[2] S. Senthilkumar, *Mechanochemical Feedback as a Patterning Principle in Hydra Regeneration*, doctoral dissertation, Technische Universität Dresden (2026).

Pattern selection in mechanochemical model of pattern formation

Szymon Cygan

(joint work with Anna Marciniak-Czochra, Finn Münnich, Dietmar Oelz)

The freshwater polyp *Hydra* can regenerate its body axis from small tissue fragments. A localized head organizer then emerges, characterized by stable expression of the Wnt3 signaling ligand. Classical explanations use the local activation–long-range inhibition principle, implemented by an autocatalytic activator and a rapidly diffusing inhibitor [1]. However, the molecular identity of the inhibitor remains unclear. Experiments instead reveal positive feedback between tissue stretching and Wnt signaling: stretching promotes morphogen production, while the morphogen changes tissue elasticity [2]. Thus a global mechanical constraint may replace a second diffusible inhibitor.

We considered a one-dimensional reduction of a mechanochemical model for a closed elastic tissue spheroid. The reference configuration is a circle of length L, whereas the deformed configuration has length $\ell > L$. Denoting the morphogen concentration by $u(x,t)$ and the infinitesimal strain by $\varepsilon(x,t)$, the coupled system takes the form

$$\begin{aligned} u_t &= Du_{xx} + \kappa\varepsilon - \alpha u, \\ 0 &= \partial_x\big(E(u)\varepsilon\big), \\ \ell - L &= \int_0^L \varepsilon(x,t)\,dx. \end{aligned} \tag{1}$$

The equations describe morphogen dynamics, instantaneous elastic equilibrium, and conservation of total strain, the source of the effective long-range interaction. For $E(u) = e^{-\beta u}$, eliminating the mechanical variable and nondimensionalizing yields the scalar nonlocal equation

$$u_t = Du_{xx} - u + \kappa \frac{e^u}{\displaystyle\int_{\mathbb{T}} e^u\,dy}, \qquad x \in \mathbb{T}, \tag{2}$$

with periodic boundary conditions. Here $\mathbb{T}$ is the circle of unit length. The nonlocal denominator encodes mechanical long-range inhibition, whereas the exponential numerator represents local positive feedback.

Equation (2) is globally well posed, possesses the homogeneous stationary state $U \equiv \kappa$, and drives the total mass toward κ. A central feature of the exponential coupling is the gradient-flow structure associated with

$$\mathcal{J}(u) = \frac{D}{2}\int_{\mathbb{T}} |u_x|^2\,dx + \frac{1}{2}\int_{\mathbb{T}} |u|^2\,dx - \kappa \log\left(\int_{\mathbb{T}} e^u\,dx\right). \tag{3}$$

Variational arguments show that, for every $\kappa > 0$, nonconstant stationary solutions exist when diffusion is sufficiently small. A minimizer of $\mathcal{J}$ then provides a Lyapunov-stable patterned state. In contrast, for sufficiently large diffusion the functional is globally convex, the homogeneous state is the only stationary solution, and it is globally asymptotically stable.

Comparison of the nonlocal linearization with a periodic Sturm–Liouville problem shows that every stationary solution with two or more peaks is linearly and nonlinearly unstable. Hence any stable nonconstant pattern must be unimodal. The mechanical constraint selects a single localized morphogen maximum, unlike classical reaction–diffusion systems that may support several stable peaks.

The homogeneous branch also undergoes a sequence of pitchfork bifurcations at

$$\kappa_n = 1 + 4\pi^2 n^2 D, \qquad n \in \mathbb{N}.$$

The bifurcation at κ_n is subcritical when $\kappa_n < 3/2$ and supercritical when $\kappa_n > 3/2$. Only the primary branch, $n = 1$, can be stable near its bifurcation point, and this occurs in the supercritical case. In the subcritical regime, global continuation implies that the primary branch has a turning point below κ_1. Numerical continuation indicates that the branch stabilizes at this fold, producing a parameter

interval in which a homogeneous state and a unimodal patterned state coexist. The complete analysis and numerical bifurcation diagrams are presented in [4].

Regenerating *Hydra* spheroids also swell and rupture periodically due to osmosis [3]. We represented this process by a time-dependent tissue length $\ell(t)$, leading formally to

$$u_t = Du_{xx} - u + \kappa\big(\ell(t) - L\big)\frac{e^u}{\displaystyle\int_{\mathbb{T}} e^u\, dy}.$$

Periodic mechanical forcing can thus move the system through distinct pattern-forming regimes. Its analysis and the extension to larger surfaces supporting several organizers remain directions for future work.

References

[1] A. Gierer and H. Meinhardt, *A theory of biological pattern formation*, Kybernetik **12** (1972), 30–39.

[2] S. L. Weevers et al., *Mechanochemical patterning localizes the organizer of a luminal epithelium*, Science Advances **11** (2025), eadu2286.

[3] M. Kücken, J. Soriano, P. A. Pullarkat, A. Ott, and E. M. Nicola, *An osmoregulatory basis for shape oscillations in regenerating Hydra*, Biophysical Journal **95** (2008), 978–985.

[4] S. Cygan, A. Marciniak-Czochra, F. Münnich, and D. Oelz, *Stability and bifurcation analysis in a mechanochemical model of pattern formation*, arXiv:2602.09998 [math.AP] (2026).

Singular patterns & ecosystem resilience

Arjen Doelman

1. The evasion of tipping & pattern forming mechanisms

'Tipping', i.e. the catastrophic collapse of an ecosystem is typically predicted in the setting of low-dimensional ODE models [8]. However, it was shown recently in [7] that if one allows for spatial effects, i.e. if one extends the ODE models to PDEs, the saddle-node bifurcation associated to tipping may be preceded by a pattern forming Turing bifurcation. The vegetation patterns generated by the Turing bifurcation may persist beyond the tipping/saddle-node point: instead of collapsing (typically to a bare soil state), the ecosystem may be more resilient. In other words, by forming patterns it may evade collapse.

The increase of resilience, i.e. the capacity of a ecosystem to adapt to changing circumstances without collapsing, is a mathematical phenomenon: it may appear in any spatially extended complex system. Moreover, the multi-stability associated to patterns is the driving mechanism, however, these patterns need not be initiated by a Turing bifurcation. In [4] it was shown numerically for a dryland ecosystem model that bare soil fronts that invade into homogeneously vegetated areas are unstable with respect to a transversal sideband, also called 'fingering', instability. The 'fingers' generated by this instability counter-invade the bare soil state. Eventually, the ecosystem reaches a patterned endstate that is resilient against further changes – due to the multi-stability associated to the patterns.

The inclusion of spatially inhomogeneous effects, such as induced by the topography of a domain/ecosystem, is a third pattern generating mechanism, and thus a third means by which an ecosystem/a complex system may evade tipping [1].

2. Singularly perturbed 2-component reaction-diffusion equations

Typical ('conceptual') ecosystem models that generate the kind of dynamics discussed above are given by systems of singularly perturbed 2-component reaction-diffusion equations,

$$\left\{ \begin{array}{rcl} \tau U_t &=& \Delta U + F(U,V;\vec{\mu}) \\ V_t &=& \frac{1}{\varepsilon^2}\Delta V + G(U,V;\vec{\mu}) \end{array} \right. \tag{1}$$

with $U(x,y,t), V(x,y,t) : \mathbb{R}^2 \times \mathbb{R}^+ \to \mathbb{R}$, $F(U,V;\vec{\mu}), G(U,V;\vec{\mu}) : \mathbb{R} \times \mathbb{R} \times \mathbb{R}^m$ ($m \geq 1$) sufficiently smooth, and $0 < \varepsilon \ll 1$, an asymptotically small parameter that measures the ratio of the spreading rates between water and biomass, or grasses and trees. Here, we impose the further simplifications: $U(x,t), V(x,t) : \mathbb{R} \times \mathbb{R}^+ \to \mathbb{R}$ and $\tau = 1$. Moreover, we assume that the system is spatially homogeneous, i.e. that neither $F(U,V)$ nor $G(U,V)$ depends explicitly on space x and that the parameters $\vec{\mu} \in \mathbb{R}^m$ also are constant throughout the domain/ecosystem.

It follows by a very direct (Fourier-based) approach that if a background state $(\bar{U}(\mu), \bar{V}(\mu))$ undergoes a saddle-node bifurcation at $\mu = \mu^*$, the spatially homogeneous ODE associated to PDE (1) undergoes tipping if $F^*_U + G^*_V < 0$ (with $F^*_U = \frac{\partial F}{\partial U}(\bar{U}(\mu^*), \bar{V}(\mu^*); \mu^*)$, etc.) and that tipping evasion may be possible if there is a Turing bifurcation preceding the tipping point, i.e. if additionally $F^*_U + \varepsilon^2 G^*_V > 0$ [7].

Based on the methods of *Geometric Singular Perturbation Theory* [6] it has been shown in [3] that the typical dryland models considered in the literature indeed exhibit invasion fronts and that these fronts are unstable with respect to the fingering instability, i.e. it is shown in [3] that invasion fronts initiate fingering patterns.

3. Inhomogeneous systems

Perhaps the most simple inhomogeneous reaction-diffusion model is the (scalar) Allen-Cahn model, $U_t = U_{xx} + U - U^3 + \varepsilon f(U, U_x, x)$. Stationary patterns correspond to a driven planar Hamiltonian system, $u_{xx} + u - u^3 = -\varepsilon f(U, U_x, x)$, which typically exhibits horse shoes and chaotic solutions if f is a periodic function of x [5]. Although these solutions are unstable in the ODE, it is shown in [1] that these orbits correspond to patterns that may be stable as solution of the PDE. More in general, it is shown in [1] that even small spatial heterogeneities generate rich families of patterns: they increase the resilience of a complex system.

4. Conclusions

The mathematical methods and ideas developed and discussed in the context of ecosystems have direct impact beyond 'just' ecosystems. For instance, it is shown

in [2] that the same instability that drives the appearance of 'fingers' in ecosystems may distinguish between benign and malignant (cancerous) tumors.

References

[1] R. Bastiaansen, A. Doelman, T.J. Kaper, *Multi-front dynamics in spatially inhomogeneous Allen-Cahn equations*, Physica D **489** (2026), 135139.

[2] P. Carter, A. Doelman, P. van Heijster, D. Levy, P. Maini, E. Okey, P. Yueng, *Deformations of acid-mediated invasive tumors in a model with Allee effect*, J. Math. Biology **90**(6) (2025), 55.

[3] P. Carter, A. Doelman, K. Lilly, E. Obermayer, S. Rao, *Criteria for the (in)stability of planar interfaces in singularly perturbed 2-component reaction-diffusion equations*, Physica D **444** (2023), 133596.

[4] C. Fernandez-Oto, O. Tzuk, E. Meron, *Front instabilities can reverse desertification*, Phys. Rev. Lett. **122** (2019), 048101.

[5] J. Guckenheimer, P. Holmes, *Nonlinear Oscillations, Dynamical Systems, and Bifurcations of Vector Fields*, *Applied Mathematical Sciences* **42** Springer (2002).

[6] C.K.R.T. Jones, *Geometric Singular Perturbation Theory*, in: R. Johnson (Ed.), *Dynamical Systems, Montecatibi Terme, 1994*, in: *Lecture Notes in Mathematics* **1609**, Springer, 1995.

[7] M. Rietkerk, R. Bastiaansen, S. Banerjee, J. van de Koppel, M. Baudena, A. Doelman, *Evasion of tipping in complex systems through spatial pattern formation*, Science **374** (2021), eabj0359.

[8] M. Scheffer, S. Carpenter, J. A. Foley, C. Folke, B. Walker, *Catastrophic shifts in ecosystems*, Nature **413** (2001), 591–596.

Mechanochemical pattern formation: far-from-equilibrium patterns on a deforming surface

Frits Veerman

Mechanochemical interaction, defined as the active interplay between a dynamical surface and a morphogen diffusing on that surface, can lead to spontaneous pattern formation. As the substrate surface plays the role of the long-range inhibitor, mechanochemical interaction can serve as an alternative to the dominant Turing paradigm when the identification of an inhibitor is problematic. I will present a paradigmatic model class for mechanochemical interaction, and will show the emergence of far-from-equilibrium patterns for a range of parameter values when specific interaction functions are chosen. These analytical results are obtained using Geometric Singular Perturbation Theory, a technique that uses time scale separation in higher-dimensional dynamical systems to reduce the system complexity, and thereby allowing us to constructively prove the existence of specific orbit types (homoclinic, heteroclinic, periodic). In addition, I will discuss recent developments in a mechanochemical model for septin binding on GUVs (giant unilamellar vesicles), where the local septin orientation can determine and predict experimentally observed surface patterns.

Conical Surface Minimizers in Variational Models of Biofilms

Blanch-Mercader, Carles

(joint work with D. J. G. Pearce, C. Thibault, Q. Chaboche. Experimental results in the second part are due to T. L. A. Nguyen, F. C. Tsai)

The study of shape-shifting materials, often inspired by biological systems, has led to a wide range of applications. Notable examples include deformable solids endowed with prescribed orientational fields, such as elastomers or inflatable structures. In such solid-based models, out-of-plane deformations arise from relaxing elastic stresses tied to a fixed orientational field. However, these models miss key features of many biological tissues, such as collective flows and dynamic reorganisation of orientational order. Motivated by this, we focus on fluid membranes endowed with nematic orientational order. Unlike solid systems, nematic membranes can flow, remodel, and continuously adapt both their geometry and orientation in response to internal stresses and external perturbations. These additional features fundamentally modify the coupling between shape and order, enabling deformation modes unavailable in solid materials.

In the first part of the talk, I presented a minimal model of a fluid membrane with nematic orientational order and addressed the question: what are the minimal-energy configurations generated by a +1 integer topological defect when both geometry and orientational order can relax freely? Our analysis was restricted to configurations exhibiting rotational symmetry with the outer circular boundary held at a fixed radius R. The nematic orientational order was described by a director field $\hat{\mathbf{n}}$, which was a unit vector tangent to the surface, with the identification $\hat{\mathbf{n}} \sim -\hat{\mathbf{n}}$. Since we focus on rotationally symmetric configurations, the director field forms a +1 topological defect at the membrane's centre $r = 0$.

The two-dimensional free-energy of the membrane is given by

$$\mathcal{F} = \int_{\mathcal{A}} \Big\{ k_B \mathcal{H}^2 + \sigma + k_1 (\nabla \cdot \hat{\mathbf{n}})^2 + k_2 (\hat{\mathbf{n}} \cdot (\nabla \times \hat{\mathbf{n}}))^2 + k_3 (\hat{\mathbf{n}} \times (\nabla \times \hat{\mathbf{n}}))^2 \Big\} \mathrm{d}a. \tag{1}$$

The first term in the free-energy expression corresponds to the bending energy, characterised by the mean curvature $\mathcal{H}$. The second term accounts for the surface tension. The remaining terms correspond to the two-dimensional effective Frank free-energy of an achiral nematic liquid crystal, as derived in [1]. The operators ∇ in Eq. (1) denotes the surface gradient, obtained by projecting the three-dimensional gradient onto the tangent plane of the surface. From left to right, these contributions are associated with splay, twist, and bend distortions of the director field. The corresponding elastic coefficients are the bending rigidity k_B, the surface tension σ, and the reduced Frank constants k_1, k_2, and k_3, which scale with the membrane thickness. In this talk, we focused on the special case of the one-constant approximation, where $k_1 = k_2 = k_3 = k$.

We first used Monte Carlo methods to obtain equilibrium configurations of Eq. (1). The length scale is set by $R = 1$, and the energy scale by $k + k_B + \sigma = 1$. Figure 1a shows the phase diagram of the surface height at the center $r = 0$, $z(r = 0)$, as the elastic constants k, k_B, and σ are varied.

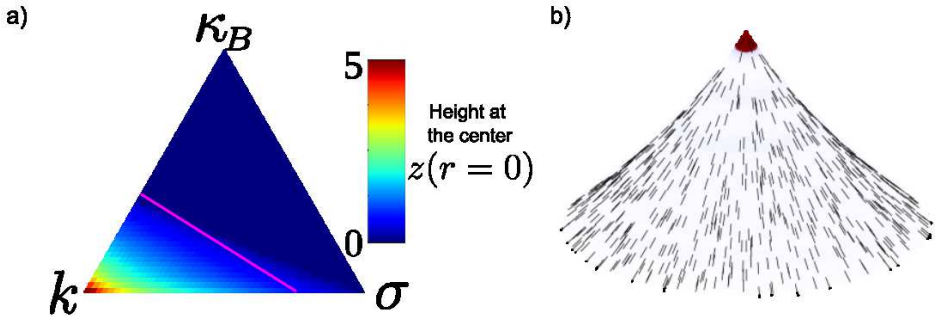

FIGURE 1. **(a)** Phase diagram of the surface height at the center, $z(r = 0)$, as a function of the reduced Frank constant k, the surface tension σ, and the bending rigidity k_B, under the constraint $\sigma + k_B + k = 1$. Magenta line: formula obtained by approximating the equilibrium state by a conical surface with an aster. **(b)** Example of an equilibrium state. Black lines: director field $\hat{\mathbf{n}}$.

When either the bending rigidity, $k_B \gg k$, or the surface tension, $\sigma \gg k$, is much larger than the reduced Frank constant, the equilibrium states are flat discs, $z(r = 0) = 0$ (Fig. 1a). In the opposite regime, when $k \gg k_B$ and $k \gg \sigma$, the equilibrium state instead becomes an approximately conical surface with a finite height, $z(r = 0) \neq 0$ (see Fig. 1a-b). The transition from a flat disc to a conical surface occurs at a finite threshold value of the reduced Frank constant k relative to the other two elastic parameters (see Fig. 1a, pink line).

To understand the flat-to-conical bifurcation, we analytically solved the normal force-balance equation from Eq. (1) for the special case of $\sigma R^2/k_B = 0$ and a director field with constant phase ψ. In this case, conical surfaces constitute a family of exact solutions, even when the one-constant approximation is relaxed, whose minimizer phase corresponds to that of an aster $\psi = 0$. In the regime $\sigma R^2/k_B \neq 0$, we approximate the equilibrium solutions by a conical surface with an aster, from which we obtained a bifurcation condition in good agreement with numerics, especially near $\sigma R^2/k_B = 0$ (Fig. 1a, pink line).

In the second part of the talk, I presented preliminary experiments on actin films on vesicles. Based on estimates of the elastic parameters, we hypothesised that the vesicles undergo morphological transitions between spherical and dendritic phases. Experimental results showed that tubular protrusions can emerge at topological defect sites in the actin films.

The first part of the talk discussed results published in Ref. [2].

REFERENCES

[1] G. Napoli, and L. Vergori. *Extrinsic curvature effects on nematic shells*, Phys. Rev. Lett, **108** (2012), p.207803.

[2] D.J.G. Pearce, C. Thibault, Q. Chaboche, and C. Blanch-Mercader, *Passive defect driven morphogenesis in nematic membranes*, Phys. Rev. Lett., **134** (2025).

Stability and Bifurcations in a Free Boundary PDE Models of Cell Motility

Leonid Berlyand

(joint work with Oleksii Krupchytskyi, Tim Laux, Volodymyr Rybalko, Alex Safsten, Elina Soskina)

We begin with a brief overview of the rapidly developing research area of active matter (a.k.a. active materials). These materials are intrinsically out of equilibrium resulting in novel physical properties whose modeling requires the development of new mathematical tools. We focus on studying the onset of motion of a living cell (e.g., a keratocyte) driven by myosin contraction. We introduce a minimal two-dimensional free-boundary PDE model that captures the evolution of the cell shape and nonlinear diffusion of myosin.

Firstly, we consider a linear diffusion model with two sources of nonlinearity: Keller-Segel cross-diffusion term and the free boundary that models moving or deformable cell membranes. Here we establish asymptotic linear stability and derive the explicit formula for the stability-determining eigenvalue.

Secondly, we consider the effect of nonlinear myosin diffusion, which results in the change of the bifurcation type from super- to subcritical, and obtain an asymptotic representation of the bifurcation curve (for small velocities). This allows us to derive an explicit formula for the curvature at the bifurcation point that controls the bifurcation type. In the most recent work in progress with the Heidelberg biophysics group, we study the relation between various types of nonlinear diffusion and bistability.

Furthermore, we discuss novel mathematical features of this free boundary model with a focus on non-self-adjointness, which plays a key role in the spectral stability analysis. Our mathematics reveals the physical origins of the non-self-adjoint of the operators in this free boundary model.

Finally, we discuss the work in progress which concerned with the second bending point of the bifurcation diagram and the rigorous mathematical proof of bistability, that is the coexistence of the stationary and a traveling wave solution in the same range of physical parameters. We present two approaches to establish the existence of a bending point with finite velocity that is different from the bifurcation point at zero velocity. Namely, we i) perform higher order asymptotic analysis in small velocities and ii) establish global bifurcation results and use Leray–Schauder degree degree theory. These results are supported by the numerical study, where the existence and asymptotic formulas characterizing such bending points, as well as bistability are verified.

References

[1] L. Berlyand, O. Krupchytskyi, T. Laux, *Change of bifurcation type in 2D free boundary model of a moving cell with nonlinear diffusion*, Journal of Nonlinear Science **36**(2026), 95.

[2] L. Berlyand, C. Alex Safsten, L. Truskinovsky, *Nonlinear stability in a free boundary model of active locomotion*, Archive for Rational Mechanics and Analysis **250** (2026), 2.

[3] L. Berlyand, V. Rybalko, *Emergence of traveling waves and their stability in a free boundary model of cell motility*, Transactions of the AMS, Vol 376, No. 3, pp. 1799-1844 (2023).
[4] L. Berlyand, C. A. Safsten, V. Rybalko, *Asymptotic stability of contraction-driven cell motion*, Physical Review E. Vol. 105, Issue 2, 024403 (2022).
[5] L. Berlyand, O, Krupchytskyi, T. Laux, C. A. Safsten, E. Soskina, *Saddle-Node Bifurcation and Spectral Stability of Traveling Waves in a Free-Boundary Cell Motility Model*, (in preparation)

Numerysis: A numerical–analytic route to rigorous bistability in a cell-motion model

Alex Safsten
(joint work with Leonid Berlyand, Oleksii Krupchytskyi, Tim Laux, Elina Soskina)

We consider a two-dimensional free-boundary model for crawling cell motion in which contractile myosin dynamics are coupled to mechanical stress and motion of the cell membrane. The cell occupies a time-dependent domain $\Omega(t) \subset \mathbb{R}^2$, with myosin density m and stress σ. In nondimensional form,

$$Z\Delta\sigma = \sigma - Pm, \qquad \partial_t m = \nabla\cdot\big(D(m)\nabla m - Km\nabla\sigma\big) \quad \text{in } \Omega(t),$$

with $\partial_\nu m = 0$, $\sigma = -\gamma H + 1 - |\Omega(t)|$, and $K\partial_\nu\sigma = V_\nu$ on the boundary, together with $\int_{\Omega(t)} m = 1$. We use $D(m) = m_\infty^2/(m_\infty - m)^2 - e_A m$, where e_A is a cooperative binding parameter. Earlier work established bifurcation of traveling waves from radially symmetric stationary cells and their stability near bifurcation; see [3, 1]. Our goal is to prove that, for the same parameter value K, a stable stationary cell and a stable traveling cell can coexist.

Let V denote traveling-wave velocity and write the branch as $K = K(V, e_A)$. Reflection symmetry makes this function even in V, so

$$K(V, e_A) = K_0 + K_2(e_A)V^2 + K_4(e_A)V^4 + O(V^6). \tag{1}$$

The sign of K_2 determines whether the pitchfork is locally supercritical or subcritical. For the nonlinear diffusion above, the formula in [1] shows that K_2 is a rational function of e_A and changes sign. When $K_2 < 0$, the traveling-wave branch initially enters the parameter region where the stationary state remains stable. Bistability can therefore occur if the branch bends back and the traveling waves change stability.

The bend is forced by a double-asymptotic argument. Merely knowing $K_2 < 0 < K_4$ at one parameter value is insufficient because higher-order terms could prevent a turning point. Instead, if for some e_A^*

$$K_2(e_A^*) = 0, \qquad K_2'(e_A^*) < 0, \qquad K_4(e_A^*) > 0, \tag{2}$$

then for $e_A > e_A^*$ sufficiently close to e_A^* there is a small $V_* > 0$ for which $\partial_V K(V_*, e_A) = 0$ and $\partial_V^2 K(V_*, e_A) > 0$. Very close to $V = 0$ the small negative quadratic term dominates, while on a slightly larger velocity scale the positive quartic term dominates before the higher orders take over.

The branch geometry is linked to stability by the bifurcation eigenvalue theorem of Crandall and Rabinowitz [2]. If $\mu(K)$ and $\lambda(V)$ denote the leading eigenvalues along the stationary and traveling branches, respectively, previous analysis gives $\mu'(K_0) > 0$ and

$$\lim_{V\to 0} \frac{VK'(V)\mu'(K_0)}{\lambda(V)} = -1, \quad \lambda_2 = -2K_2\mu'(K_0), \quad \lambda_4 = -4K_4\mu'(K_0) \text{ if } K_2 = 0.$$

Thus the same double asymptotics force a sign change of the leading traveling-wave eigenvalue. A stable portion of the folded traveling-wave branch then overlaps in K with the stable stationary branch.

It remains to verify (2) for the PDE. We expand m, σ, and the free boundary in powers of V and angular Fourier modes. At each order the radial coefficients solve coupled Poisson–Helmholtz equations involving $\mathcal{L}_k u := u'' + r^{-1}u' - k^2 r^{-2}u$, with forcing and boundary data coming from lower orders. In the first Fourier mode an extra boundary condition becomes a solvability condition. For even n this yields

$$K_n = \frac{A_n + \int_0^{R_0} f_n(r)\, dr}{B_n + \int_0^{R_0} g_n(r)\, dr}, \tag{4}$$

where the right-hand side depends only on fields of order at most n. This gives an effective route to K_2 and K_4, but the fourth-order forcing terms are too complicated for a direct sign calculation.

This is where "numerysis" enters. Floating-point computations first locate a physically plausible regime. For $P = 0.004$, $Z = 0.075$, $\gamma = 0.0025$, and $m_\infty = 10$, a transition occurs numerically near $e_A = 0.55599$, with $K_2 \approx 0$, $\partial_{e_A} K_2 \approx -1.15 \times 10^3$, and $K_4 \approx 330$. We replace every approximate quantity by a certified interval: zero-order parameters by validated root calculations, Bessel functions by rigorous series bounds, and radial Poisson–Helmholtz solutions by piecewise polynomials with residual and Green-function error bounds. Propagating these enclosures through (3) gives, at $e_A = 0.56$,

$$K_2 \in [-6.17, -4.17],$$

so the subcritical sign is rigorously certified.

At the time of the talk the computer-assisted proof was still in progress. The remaining target is to certify $K_4 > 0$ on an e_A-interval across which K_2 changes sign. Continuity would then produce an exact e_A^* satisfying (2), hence a rigorous bistability result. In this way numerical exploration identifies the regime, bifurcation theory reduces the PDE problem to scalar inequalities, and interval analysis certifies them.

References

[1] L. Berlyand, O. Krupchytskyi, and T. Laux, *Change of bifurcation type in 2D free boundary model of a moving cell with nonlinear diffusion*, J. Nonlinear Sci. **36** (2026), Article 95.

[2] M. G. Crandall and P. H. Rabinowitz, *Bifurcation, perturbation of simple eigenvalues, and linearized stability*, Arch. Rational Mech. Anal. **52** (1973), 161–180.

[3] C. A. Safsten, V. Rybalko, and L. Berlyand, *Asymptotic stability of contraction-driven cell motion*, Phys. Rev. E **105** (2022), 024403.

Active Solitons

Lev Truskinovsky

In many biological systems, localized mechanical information is transmitted by mechanically neutral chemical signals. Typical examples include contraction waves in the actomyosin cortex at the cellular scale, and peristaltic waves at tissue level. In such systems, chemical activity is transformed into mechanical deformation by distributed motor-type mechanisms. To elucidate the underlying principles of chemo-mechanical coupling, we presented in this talk the simplest example of a directional motion in a distributed mechanical system, guided by a purely chemical cue. It shows that localized mechanical signals can be driven by chemical activity in a highly efficient manner.

More specifically, we have shown that chemo-mechanical driving of localized solitary waves (solitons, for simplicity) can be mechanically efficient in the sense that the mechanical energy needed to activate the pulse at the leading edge can be mechanically transported from the trailing edge where it is released due to the pulse closure. Such self-sustaining machinery can be operated due to the existence of a mechanism of an internal energy transport through wave dispersion. We have shown how exactly, due to an onboard energy-harvesting, the mechanical signals generated in these regimes can propagate without taking any energy from the triggering chemical waves.

In this talk we focused on the mechanical side of the implied energy transport without invoking in any detail the underlying chemical machinery. Our main technical tool was the theory of dispersive systems. We built on the theoretical ideas developed in the description of defects in crystals, which can produce lattice-scale energy radiation and can also be guided by lattice waves.

The obtained pulse solutions can be interpreted as describing spatially distributed chemo-mechanical motors converting mechanically neutral chemical signals into functional mechanical activity. An example of such phenomenon is peristalsis by actively generated waves of muscle contraction. We show that peristalsis can be modeled by a train of rectangular-shaped solitary waves of localized activity propagating through otherwise passive matter, the obtained solitary wave solutions were extended as periodic nonlinear waves which could already be used directly to model the peristaltic mode of self propulsion.

References

[1] N. Gorbushin and L. Truskinovsky, *Peristalsis by pulses of activity*, Phys. Rev. E **103** (2021), 042411.

[2] L. Truskinovsky and G. Zurlo, *Active chemo-mechanical solitons*, Phys. Rev. E **113** (2026), 034215.

Reporter: Emanuel Eitel

Participants

Prof. Dr. Leonid Berlyand
Department of Mathematics
Pennsylvania State University
843 Wheatfield Dr
State College PA 16802
UNITED STATES

Dr. Carles Blanch-Mercader
Institut Curie
Section Research, UMR 168
11, rue Pierre et Marie Curie
75005 Paris Cedex 05
FRANCE

Dr. Szymon Cygan
Mathematisches Institut
Universität Heidelberg
Im Neuenheimer Feld 205
69120 Heidelberg
GERMANY

Prof. Dr. Arjen Doelman
Mathematisch Instituut
Universiteit Leiden
Postbus 9512
2300 RA Leiden
NETHERLANDS

Emanuel Eitel
Institut für Mathematik
Universität Heidelberg
Im Neuenheimer Feld 205
69120 Heidelberg
GERMANY

Fabius Krämer
Institut für Mathematik
Universität Heidelberg
Im Neuenheimer Feld 205
69120 Heidelberg
GERMANY

Prof. Dr. Tim Laux
Institut für Mathematik
Universität Heidelberg
Im Neuenheimer Feld 205
69120 Heidelberg
GERMANY

Prof. Dr. Anna Marciniak-Czochra
Institut für Mathematik
Universität Heidelberg
Im Neuenheimer Feld 205
69120 Heidelberg 69120
GERMANY

Marko Popovic
Max Planck Institute for the Physics of
Complex Systems
Nöthnitzer Straße 38
01187 Dresden
GERMANY

Prof. Dr. Keith Promislow
Department of Mathematics
Michigan State University
C212 Wells Hall, 619 Red Cedar Road
East Lansing, MI 48824-1027
UNITED STATES

Dr. Alex Safsten
University of Maryland
4176 Campus Drive
College Park, MD 20742-4015
UNITED STATES

Prof. Dr. Markus Schmidtchen
Fakultät Mathematik
Technische Universität Dresden
Zellescher Weg 25
01069 Dresden
GERMANY

Prof. Dr. Ulrich Schwarz
Institut für Theoretische Physik
Universität Heidelberg
Philosophenweg 19
69120 Heidelberg
GERMANY

Prof. Dr. Angela Stevens
Institut für Analysis und Numerik
Universität Münster
Einsteinstraße 62
48149 Münster
GERMANY

Prof. Dr. Lev Truskinovsky
Physique et Mecanique des Milieux
Heterogenes
CNRS – UMR 7636
ESPCI ParisTech
10 Rue Vauquelin
75005 Paris
FRANCE

Dr. Frits Veerman
Mathematisch Instituut
Universiteit Leiden
Einsteinweg 55
2333 CC Leiden
NETHERLANDS